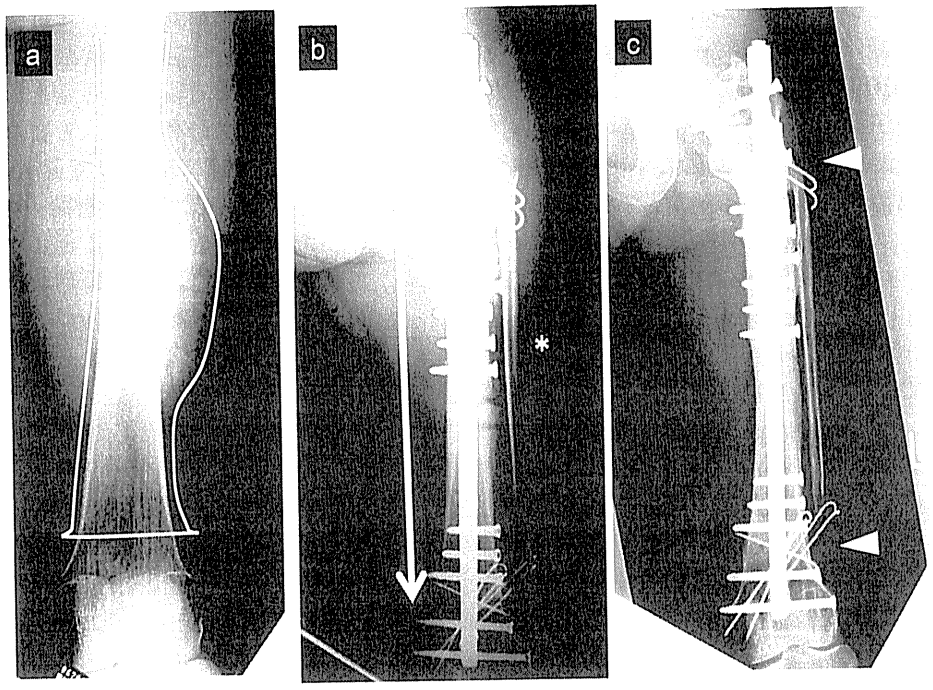

図4　体外自家照射骨による再建術例（19歳　女）

a. 左大腿部骨幹部の骨肉腫に対して広範切除を行った（白線枠）。
b. 摘出した骨から腫瘍部分を取り除き，60Gyの一括照射による殺細胞処理を行った。その後，照射骨を大腿骨欠損部に戻し，髄内釘で固定した（両矢印の範囲）。骨癒合促進のため血管柄付き腓骨移植（＊）も併用した。
c. 術後6年で，骨癒合は完成している（△は骨接合部の癒合を示す）。

吸器外科と連携のうえ，積極的な外科治療を行う必要がある。

Ⅳ 最 後 に

当科における過去50年の骨肉腫の治療成績を検討し，生存率の向上，生体材料や手術技術の進歩によって患肢温存手術が主体となっていることが確認された。しかし，骨肉腫は，稀な疾患であり，他の癌腫のようには有効な新規抗癌剤や分子標的薬の開発が進んでおらず，生存率に関しては，ここ数年は頭打ち状態の感がある。本邦では，現在，JCOG骨・軟部腫瘍グループの主導で，骨肉腫補助化学療法におけるIFM併用の有効性に関する他施設共同臨床研究が進められているが，臨床的には，限られた既存薬剤で，いかに効率よく治療効果があげて生存率を改善することができるか，ということが模索されているのが現状である。今後，生存率をさらに向上させるためには，やはり新規抗癌剤の開発を押し進めることが必要である。

参 考 文 献

1) Raymond AK, Ayala AG, Knuutila S. Conventional osteosarcoma: Pathology & Genetics. Tumors of Soft Tissue and Bone. Flecher CDM, Unii KK, Mertens F, eds. p56-57. IARC Press. 2002.
2) 上田孝文，荒木信人，吉川秀樹: 骨肉腫に対する集学的治療体系の進歩と今後の治療戦略　化学療法を中心に．小児がん. 46:175-180, 2009.
3) 横山良平: 【固形腫瘍の新しい治療】 骨肉腫の治療. 小児科診療67: 615-619, 2004.
4) 守田哲郎: 【がん化学療法の現状】 骨軟部肉腫に対する化学療法の現状. 新潟がんセンター病医誌. 37: 37-42, 1998.
5) 大塚寛，守田哲郎，堀田利雄,他: 化学療法を開始した昭和52年以降の骨原発悪性腫瘍の治療成績. 新潟整外研会誌. 11: 93-96, 1995.
6) Iwamoto Y, Tanaka K, Isu K, et al. : Multiinstitutional phase II study of neoadjuvant chemotherapy for osteosarcoma (NECO study) in Japan: NECO-93J and NECO-95J. J Orthop Sci. 14:397-404, 2009.
7) 守田哲郎: 骨原発性悪性骨腫瘍の治療. 新潟がんセンター病医誌. 33: 1-8, 1998.
8) 松本誠一: 骨肉腫の手術療法. 小児がん. 46:181-183, 2009.
9) 守田哲郎，堀田利雄，平田泰治，他: 骨原発悪性腫瘍に対する患肢温存療法 各種再建法の検討. 癌と化療. 16:1795-1801, 1989.
10) Hatano H, Ogose A, Hotta T, et al. Extracorporeal irradiated autogenous osteochondral graft: a histological study. J Bone Joint Surg Br. 87:1006-11, 2005.
11) Harting MT, Blakely ML, Jaffe N, et al. Long-term survival after aggressive resection of pulmonary metastases among children and adolescents with osteosarcoma. J Pediatr Surg. 41:194-9, 2006.

20111907A（別刷 2/2）

厚生労働科学研究費補助金

がん臨床研究事業

高悪性度骨軟部腫瘍に対する標準治療確立のための研究

平成23年度　研究成果の刊行物（別刷）

2/2

研究代表者　　岩本　幸英

平成24（2012）年　3月

厚生労働科学研究費補助金

がん臨床研究事業

高悪性度骨軟部腫瘍に対する標準治療確立のための研究

平成 23 年度　研究成果の刊行物（別刷）

2/2

研究代表者　　岩本　幸英

平成 24（2012）年　3 月

Journal of Surgical Oncology 2011;103:380–385

Prognostic Significance of HLA Class I Expression in Ewing's Sarcoma Family of Tumors

HIROKI YABE, MD,[1] TOMOHIDE TSUKAHARA, MD,[2] SATOSHI KAWAGUCHI, MD,[2]* TAKURO WADA, MD,[2] TOSHIHIKO TORIGOE, MD,[3] NORIYUKI SATO, MD,[3] CHIHIRO TERAI, MD,[1] MASAYA AOKI, MD,[4] SHIGEMICHI HIROSE, MD,[5] HIDEO MORIOKA, MD,[6] AND HIROO YABE, MD[6]

[1]*Division of Rheumatology, Jichi Medical University Saitama Medical Center, Saitama, Japan*
[2]*Department of Orthopaedic Surgery, Sapporo Medical University School of Medicine, Sapporo, Japan*
[3]*Department of Pathology, Sapporo Medical University School of Medicine, Sapporo, Japan*
[4]*Division of Clinical Laboratory, National Sanatorium Tama Zenshoen, Tokyo, Japan*
[5]*Department of Diagnostic Pathology, Keio University School of Medicine, Tokyo, Japan*
[6]*Department of Orthopaedic Surgery, Keio University School of Medicine, Tokyo, Japan*

Background: Ewing's sarcoma family of tumors (ESFT) is one of the most malignant groups of tumors in young people. Human leukocyte antigen (HLA) class I displays endogenously processed peptides to CD8+ T lymphocytes and has a key role for host immune surveillance. In ESFT, the investigation concerning both HLA class I expression and T-cell infiltration has yet to be reported.
Methods: Biopsy specimens from 28 ESFT patients were evaluated by immunohistochemistry with the anti-HLA class I monoclonal antibody (mAb) EMR8-5 and anti-CD8 mAb, respectively.
Results: Expression of HLA class I was negative in 10 tumors and down-regulated in 22 tumors. The status of CD8+ T cell infiltration was closely associated with the expression levels of HLA class I. ESFT patients with down-regulated or negative expression of HLA class I showed significantly poorer survival than the rest of the patients.
Conclusions: Our results suggested that CD8+ T cell-mediated immune response restricted by HLA class I might play an important role in immune surveillance of ESFT, and we revealed for the first time that the status of HLA class I expression affects the survival of the patients with ESFT. *J. Surg. Oncol. 2011;103:380–385.* © 2010 Wiley-Liss, Inc.

KEY WORDS: **Ewing's; sarcoma; ESFT; HLA class I; CD8; T lymphocyte**

INTRODUCTION

Ewing's sarcoma family of tumors (ESFT), consisting Ewing's sarcoma and primitive neuroectodermal tumor (PNET), represents a subset of malignant small round blue cell tumors with characteristic chromosomal translocation occurring in bone and soft tissues with a peak incidence in children and young adults [1]. Although systemic adjuvant chemotherapy has significantly improved the prognosis of patients with ESFT, disease presenting with metastatic spread or relapses after primary treatment remains incurable in the majority of cases [2,3]. This emphasizes the need for alternative treatments including immunotherapy.

Recent clinical studies have shown efficacy of immunotherapeutic strategies against various malignant tumors, where anti-tumor cytotoxic T-lymphocytes (CTL) are induced by cancer vaccination [4,5]. As anti-tumor CTL responses are elicited by the recognition of immunogenic epitopes in the context of human leukocyte antigen (HLA) class I molecules on the tumors, it is important to evaluate the status of HLA class I molecules in the ESFT tissues [6,7]. However, there is only a scarce literature available about HLA class I expression in ESFT [8].

A monoclonal antibody (mAb) against HLA class I heavy chains, EMR8-5, has been confirmed to be valid for immunohistochemistry in formalin-fixed paraffin-embedded tissues [9–12]. Using this mAb, we investigated HLA class I expression in primary lesions of ESFT patients. Furthermore, we evaluated the correlation of HLA class I expression with various clinical and histological parameters including treatment outcomes of patients and infiltration of T lymphocytes in the tumor tissues.

MATERIALS AND METHODS

The present study was approved under institutional guidelines for the use of human subjects in research and patients' specimens were analyzed after having informed written consent from the patients or their families.

Patients and Samples

Twenty-eight patients with ESFT, who had been treated in Keio university hospital between 1979 and 2009, were enrolled in this study. Follow-up period after diagnosis is 76.5 months on average (range from 10 to 275 months). Demographic data of the patients are summarized in Table I. There were 15 male and 13 female patients. The average age at diagnosis was 26.3 years (range from 1 to 70 years). Nineteen of the primary tumors arose in bone, and 9 arose in soft tissue. Fourteen tumors were located in the trunk (spine or paraspinal region in 5, chest wall in 3, and pelvis in 6 patients) and 14 tumors in the extremity. Fusion genes including EWS/FLI-1 or EWS/ERG were determined by RT-PCR in 12 out of 16 cases in which frozen biopsy specimens were available [13].

*Correspondence to: Satoshi Kawaguchi, MD, Department of Orthopaedic Surgery, Sapporo Medical University School of Medicine, South 1, West 16, Chuo-ku, Sapporo, 060-8543 Japan. Fax: 81-11-641-6026.
E-mail: kawaguch@sapmed.ac.jp

Received 20 July 2010; Accepted 16 November 2010

DOI 10.1002/jso.21829

Published online 28 December 2010 in Wiley Online Library (wileyonlinelibrary.com).

TABLE I. Clinical Characteristics of 28 ESFT Patients

Characteristics	Number
Age	
Range (average)	1–70 (26.3)
<30 Years	21
≥30 Years	7
Gender	
Male	15
Female	13
Tumor origin	
Bone	19
Soft tissue	9
Tumor site	
Extremity	14
Trunk	14
Spine or Paraspinal region	5
Chest wall	3
Pelvis	6
Tumor size	
Range (average)	4–20 (9.4)
<10 cm	12
≥10 cm	12
Stage	
IIB[a]	22
III[b]	6
Resectability of the tumor	
Resectable	23
Unresectable	5
Treatment	
Chemotherapy + surgery + radiotherapy	14
Chemotherapy + surgery	9
Chemotherapy + radiotherapy	5
Status of surgical margins	
Adequate	17
Inadequate	11

[a]Stage IIB: high-grade extracompartmental lesion, without metastasis.
[b]Stage III: any grade, with metastasis.

Size of the tumors was measured by magnetic resonance imaging in 24 patients. According to the Enneking's surgical stage [14], all the 28 patients were stratified into 22 stage IIB patients, and 6 stage III patients. Treatment consisted of chemotherapy, surgery, and radiotherapy in 14, chemotherapy and surgery in 9, chemotherapy and radiotherapy in 5 patients. Chemotherapy regimens used are VAC [15], VACA [16], CYVADIC [17], T11 [18], IFO-THP [19], VDC-IE [20,21], New A1 [22], A3 [22], and KS1 [21]. The chemotherapy regimens (KS1 and VDC-IE) containing both ifosfamide and etoposide have been used since 1995. Radiotherapy (30-65Gy) was implemented in 19 patients with unresectable tumors or those with inadequate surgical margin. The surgical margins were adequate (amputation or resection with wide margin) in 17, and inadequate (biopsy only or resection with marginal margin or intralesional margin) in 11 patients.

Immunohistochemistry

Monoclonal antibodies used were anti-HLA class I heavy chain antibody, EMR8-5 [9–12], anti-CD4 mAb (Dako, Glostrup, Denmark) and anti-CD8 mAb (Dako, Glostrup, Denmark).

Formalin-fixed paraffin-embedded sections of biopsy specimens from 28 ESFTs were deparaffinized and then boiled for 20 min in a microwave oven for antigen retrieval. The sections were blocked with 1% non-fat dry milk and stained with a streptavidin–biotin complex (Nichirei, Tokyo, Japan) as previously described [23]. The sections were then stained with hematoxylin. Positive reactivity of the EMR8-5 antibody was confirmed by staining of vascular endothelial cells and lymphocytes in sections of tumor specimens. Sections of a normal testis obtained from an autopsy specimen were used as an external negative control for immunostaining.

The reactivity of EMR8-5 was determined by staining of the plasma membranes of tumor cells. The expression status of HLA-class I was graded semiquantitatively. We classified 28 cases into three groups, high (positive cells ≥50%), low (50% > positive cells ≥5%) and negative (5% > positive cells) (Fig. 1).

Infiltrations of T cells into tumor tissues were also evaluated by semiquantitative scoring on a scale of +++ (diffuse infiltration), ++ (moderate infiltration), + (scattered or mild infiltration), and − (negative or rare) (Fig. 2).

Statistical Analysis

Disease-free survival and overall survival rates were estimated using the Kaplan–Meier plots. Both survivals were calculated from the date of initial treatment. A terminal point of disease-free survival was defined at the time of disease recurrence or progression, onset of a secondary neoplasm, death from disease, or the last review. A terminal point of overall survival was defined as the time of death or the last review. Prognostic significance of following variables on disease-free survival and overall survival was determined by univariate analysis using log-rank test [24]: age, gender, origin of tumor, tumor site, stage, surgical margin, chemotherapy regimen, status of class I HLA expression, status

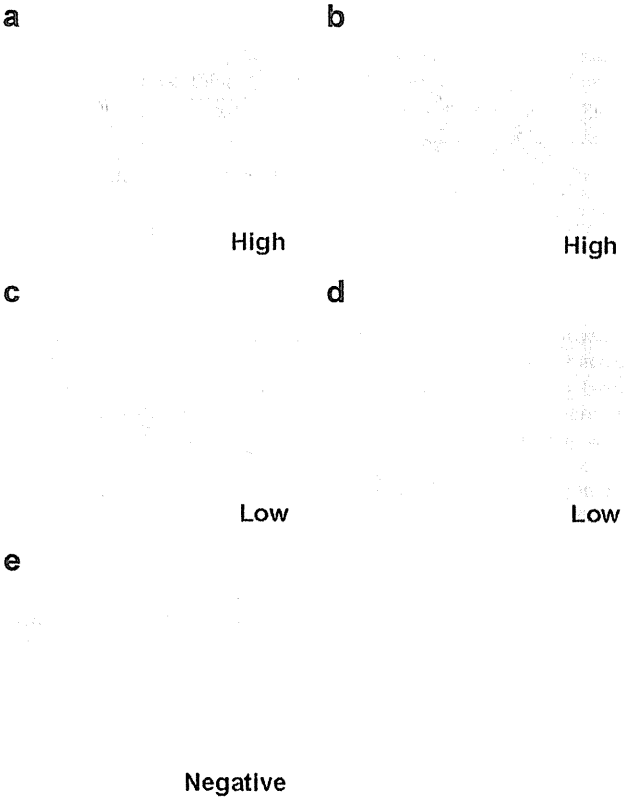

Fig. 1. Immunohistochemical grading of tumor specimens. Representative sections of ESFT specimens stained with the anti-HLA class I mAb EMR-5 are shown. **a,b**: "High" indicates a positive cell number of over 50%. **c,d**: "Low" indicates a positive cell number from 5% to 50%. **e**: "Negative" indicates that <5% of tumor cells were stained positively. Original magnification: (a), (b), (c), and (d), 200×; (e), 100×. [Color figure can be viewed in the online issue, available at wileyonlinelibrary.com.]

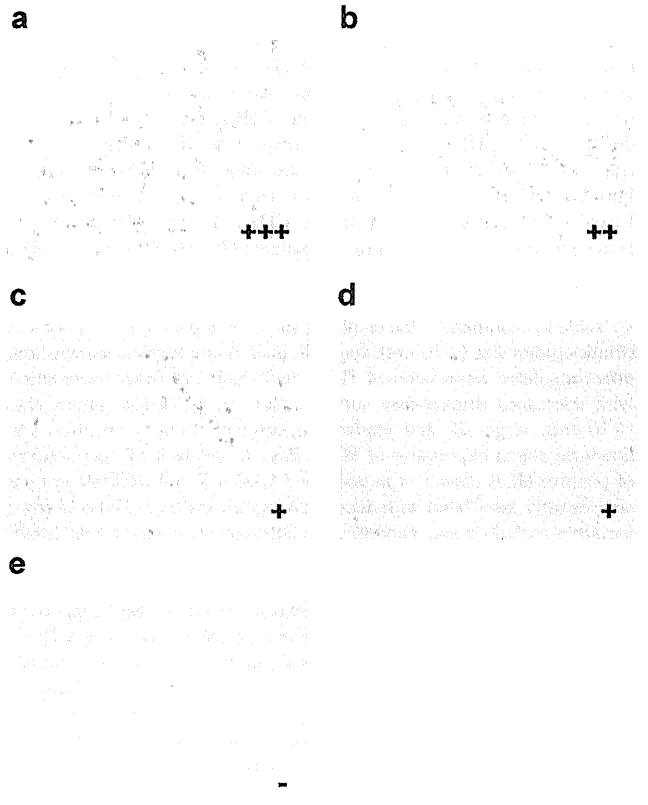

Fig. 2. Immunohistochemical grading of CD8+ T cell infiltration. Representative sections of ESFT specimens stained with an anti-CD8 mAb are shown. Infiltrations of CD8+ T cells into tumor tissues were evaluated by semiquantitative scoring. **a**: +++ (diffuse infiltration), (**b**) ++ (moderate infiltration), (**c**,**d**) + (scattered or mild infiltration), and (**e**) − (negative or rare). Original magnification: (a), (b), (c), and (d), 200×; (e), 100×. [Color figure can be viewed in the online issue, available at wileyonlinelibrary.com.]

of CD8+ T lymphocyte infiltration, and co-existence of HLA class I expression and CD8+ T cell infiltration. Subsequently a multivariate analysis was carried out for overall survival by using a Cox's proportional hazards model.

Relationship between HLA class I expression and infiltration of CD8+ T cells was statistically analyzed using Fisher's exact probability test. Clinicopathological characteristics of the patients showing HLA class I expression and CD8+ T cell infiltration were compared with those of the rest of the patients, and analyzed using Fisher's exact probability test.

All the statistical analyses were performed using JMP 8 software (SAS Institute Inc., Cary, NC). A probability of <0.05 was considered statistically significant.

RESULTS

Clinical Course of the Patients

Overall survival rate of whole 28 patients with ESFT was 53.1% in 5 years and 47.8% in 10 years, and disease-free survival rate was 38.5% in both 5 years and 10 years (Fig. 3). Local disease recurrence was seen in 11 cases. Distant metastasis was observed in 12 cases including 6 stage III cases. The sites of distant metastasis were lung in 9 patients, bone in 3, lymph nodes in 2 and other visceral organs in 1.

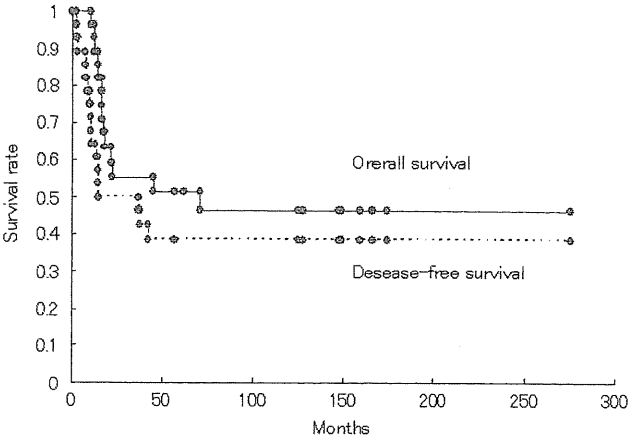

Fig. 3. Overall survival and disease-free survival of 28 patients with ESFT. Survival rates were estimated using Kaplan–Meier plots. The date of histological diagnosis was used as time 0. [Color figure can be viewed in the online issue, available at wileyonlinelibrary.com.]

Expression of HLA Class I in ESFT

To determine the phenotypic expression of HLA class I in ESFT, we stained 28 biopsy specimens of ESFT with anti-HLA class I mAb (EMR8-5). Of these, 18 specimens (64%) reacted positively with anti-HLA class I mAb where the plasma membranes of tumor cells were stained (Fig. 1). These positive cases were graded as high in 6 cases and low in 12 cases (Table II). Collectively the expression of HLA class I was lost (negative-grade expression) in 10 specimens (36%) and down-regulated (negative or low expression) in 22 specimens (79%) in ESFT.

Relationship Between HLA Class I Expression and T-Cell Infiltration in ESFTs

We then stained 28 ESFT specimens with anti-CD4 and anti-CD8 mAb. The infiltration of CD4+ T cells was seen in only two ESFT specimens (7%), whereas the infiltration of CD 8+ T cells was found in 20 specimens (71%) to various extents. Representative CD8+ T cell infiltration are shown in Figure 2. CD8+ T cell infiltration was +++ (diffuse) in 7, ++ (moderate) in 4, + (scattered or mild) in 9, and − (negative or rare) in 8 cases (Table II). The status of CD8+ T cell infiltration was closely associated with the expression levels of HLA class I ($P = 0.014$) (Table III). In the ESFT tumor tissues with positive expression of HLA class I, infiltrated CD8+ T cells tended to localize with tumor cells showing strong class I expression (Figs. 1a–c, 2a–c).

TABLE II. HLA Class I Expression and T-Cell Infiltration in 28 ESFT Specimens

High		Low	Negative
HLA class I expression			
6 (21%)		12 (43%)	10 (36%)
+++ (Diffuse)	++ (Moderate)	+ (Scattered or mild)	− (Negative or rare)
CD8+ T-cell infiltration			
7 (25%)	4 (14%)	9 (32%)	8 (29%)
CD4+ T-cell infiltration			
0	1 (4%)	1 (4%)	26 (92%)

TABLE III. Correlation Between HLA Class I Expression and CD8+ T-Cell Infiltration

	CD8+ T-cell infiltration		
HLA class I expression (n = 28)	++ or +++	− or +	*P*-value
High	5	1	0.014*
Low	5	7	
Negative	1	9	

P-value was calculated using Fisher's exact test.
*A probability of <0.05 was considered statistically significant.

Prognostic Significance of HLA Class I Expression in ESFT

Subsequently we analyzed the prognostic significance of 11 variables including expressions of HLA class I. As shown in Figure 4a, the overall survival of 18 patients with positive HLA class I expression was significantly better than that of the remaining 10 patients with negative HLA class I ($P = 0.037$). Notably, 10-year survival rate of patients with negative HLA class I was as low as 24%. In sharp contrast, all six patients with high expression of HLA class I remained alive (Fig. 4b) and continuous disease free. There were significant differences between patients with high expression of HLA class I and those with down-regulated HLA class I with respect to the overall survival (Fig. 4b; $P = 0.001$) and the disease-free survival ($P = 0.003$). Furthermore, 10 patients showing co-existence of positive HLA class I expression and moderate or diffuse CD8+ T cell infiltration had a better prognosis than the rest of the patients ($P = 0.024$) (Fig. 5). The overall survival rates of those 10 patients were 78.8% at 5 years and 10 years.

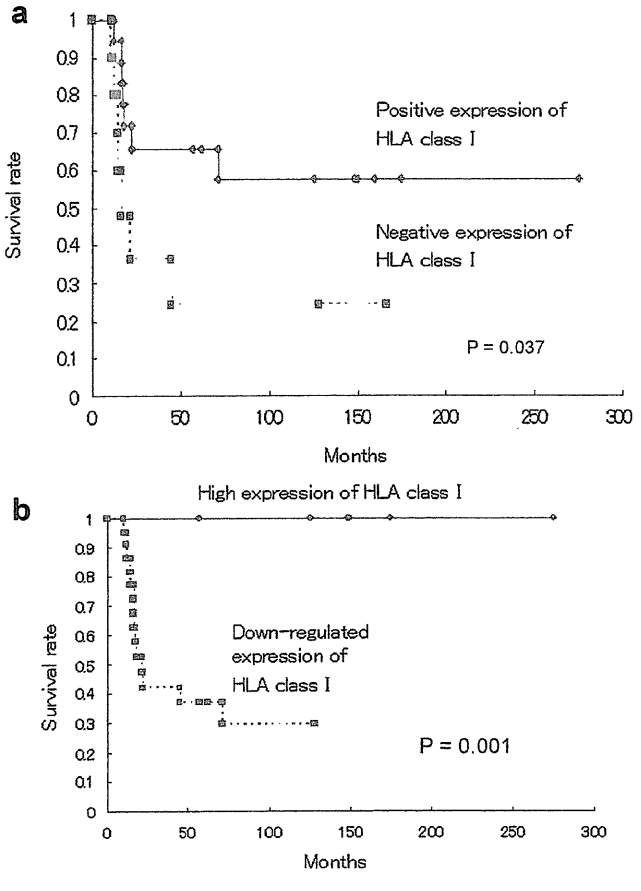

Fig. 4. Survival curves of 28 patients with ESFT stratified by HLA class I expression status. **a**: Overall survival curves. Patients were divided according to HLA class I expression status into two groups (positive (low or high) expression, n = 18; negative expression, n = 10). Survivals were estimated using Kaplan–Meier plots. *P*-value was calculated using log-rank test. **b**: Overall survival curves. Patients were divided according to HLA class I expression status into two groups (high expression, n = 6; down-regulated (negative or low) expression, n = 22). [Color figure can be viewed in the online issue, available at wileyonlinelibrary.com.]

Table IV summarizes the results of survivorship analysis. Tumor site (trunk), tumor size (≥10 cm), stage III, inadequate surgical margin, and down-regulated expression of HLA class had significant association with decreased disease-free survival. Soft tissue origin, tumor size (≥10 cm), stage III, and inadequate surgical margin, negative and down-regulated expression of HLA class I, and lack of co-existence of positive HLA class I expression and CD8+ T cell infiltration were significantly associated with decreased overall survival. None of other variables including age, gender, chemotherapy regimen, and the levels of CD8+ T cell expression showed significant association with disease-free or overall survival.

Prognostic impact of co-existence of positive HLA class I expression and CD8+ T cell infiltration was further examined by using a Cox's proportional hazards model. Given the limited sample size, the analysis included three covariate parameters in total. As shown in Table V, multivariate analysis revealed that stage III and co-existence of positive HLA class I expression and moderate or diffuse CD8+ T cell infiltration were independent prognostic factors, respectively.

Clinicopathological Characteristics of ESFTs Showing HLA Class I Expression and CD8+ T Cell Infiltration

Finally we assessed clinicopathological characteristics of 10 patients showing co-existence of positive HLA class I expression and CD8+ T-cell infiltration (Table VI). Of nine characteristics examined, tumor size (<10 cm) and absence of metastasis at the final follow-up were

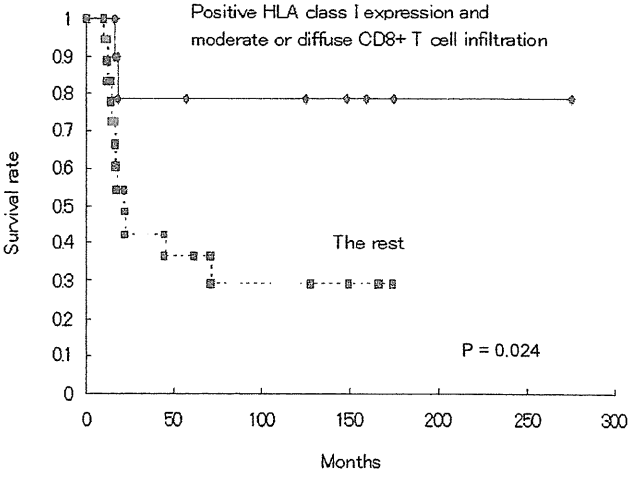

Fig. 5. Overall survival curves of 28 patients with ESFT. Patients were divided into two groups (patients showing co-existence of positive (low or high) HLA class I expression and moderate or diffuse CD8+ T cell infiltration, n = 10; patients with the other expression patterns, n = 18). Survivals were estimated using Kaplan–Meier plots. *P*-value was calculated using log-rank test. [Color figure can be viewed in the online issue, available at wileyonlinelibrary.com.]

TABLE IV. Univariate Analysis of Potential Unfavorable Prognostic Factors

Variables	Categories	No. patients	*P*-value DFS	*P*-value OS
Age (years old)	≥30 (vs. <30)	7	0.481	0.632
Gender	Female (vs. male)	13	0.515	0.679
Tumor origin	Soft tissue (vs. bone)	9	0.181	0.036*
Tumor site	Trunk (vs. extremity)	14	0.028*	0.237
Tumor size (cm)	≥10 (vs. <10)	12	0.020*	0.042*
Stage	Stage III (vs. stage IIB)	6	<0.001*	<0.001*
Surgical margin	Inadequate (vs. adequate)	11	0.008*	0.026*
Chemotherapy regimen	Not including IE (vs. including IE)	13	0.263	0.143
HLA class I expression	Negative (vs. positive)	10	0.132	0.037*
HLA class I expression	Down-regulated (vs. high)	22	0.003*	0.001*
CD8+ T-cell infiltration	− or + (vs. ++ or +++)	17	0.145	0.071
HLA class I/CD8+ T cell	Lack of co-existence of positive HLA class I expression and CD8+ T-cell infiltration (++ or +++)	18	0.067	0.024*

DFS, disease-free survival; OS, overall survival; IE, ifosfamide and etoposide.
P-value was determined by univariate analysis using log-rank test.*A probability of <0.05 was considered statistically significant.

significantly associated with co-existence of positive HLA class I expression and CD8+ T-cell infiltration. At the time of diagnosis, 22 patients were free from distant metastasis (Stage IIB). At the time of the final follow-up (76.5 months on average), all 9-stage IIB patients with co-existence of HLA class I expression and moderate or diffuse CD8+ T-cell infiltration remained free from metastasis. In contrast, 6 out of 13 stage IIB patients with lack of the co-existence had distant metastasis developed during the follow-up period.

DISCUSSION

By staining 28 biopsy specimens of ESFT treated in a single institute, we found down-regulation of HLA class I molecules in 79%, infiltration of CD4+ T cells in 7% and infiltration of CD8+ T cells in 74% of the primary tumors. Subsequent clinicopathological analysis revealed that down-regulation of HLA class I molecules was significantly associated with poor CD8+ T-cell infiltration, poor overall and event-free survival. Furthermore co-existence of positive HLA class I expression and moderate or diffuse CD8+ T-cell infiltration served as an independent significant favorable prognostic factor, and was associated with small tumor size and lack of having metastasis develop during follow-up. These findings indicated the prognostic role of HLA class I molecules in patients with ESFT, potentially through modulation of CD8+ T cell-mediated immune surveillance.

Previously Berghuis et al. [8] investigated HLA class I expression in 61 ESFT biopsy samples. Consistent with our findings, they found down-regulated expression of HLA class I in 79% of the samples. The frequency of absent HLA class I expression was as similar as 28% in their study and 36% in the present study. In contrast, in the study by Berghuis et al. [8], there is no significant impact of HLA class I expression levels on overall or event-free survival of the patients. This analysis was made on 35 out of 61 patients with ESFT. Therefore, the process of patient's selection may have influenced the prognostic significance of HLA class I expression, even though clinical pictures of these 35 patients have not been documented. Another

TABLE V. Multivariate Analysis for Overall Survival of 28 ESFT Patients

Variables	Categories	Risk ratio (95% CI)	*P*-value
Stage	Stage III	7.79 (2.09–33.18)	0.003*
Surgical margin	Inadequate	2.51 (0.83–8.48)	0.104
HLA class I/CD8+ T cell	Lack of co-existence of positive HLA class I expression and CD8+ T cell infiltration (++ or +++)	4.81 (1.28–31.44)	0.018*

95% CI, 95% confidence interval.
P-value was determined by Cox regression analysis.
*A probability of <0.05 was considered statistically significant.

TABLE VI. Clinicopathological Characteristics of 10 Patients Showing HLA Class I Expression and CD8+ T-Cell Infiltration

Characteristics	HLA class I expression and CD8+ T-cell infiltration (++ or +++) Yes (n = 10)	No (n = 18)	*P*-value
Age (years)			
<30	7	14	0.491
≥30	3	4	
Gender			
Male	6	9	0.456
Female	4	9	
Tumor origin			
Bone	8	11	0.278
Soft tissue	2	7	
Tumor site			
Extremity	5	9	0.653
Trunk	5	9	
Tumor size (cm)[a]			
<10	7	5	0.014*
≥10	1	11	
Stage			
Stage IIB	9	13	0.277
Stage III	1	5	
Surgical margin			
Adequate	6	11	0.632
Inadequate	4	7	
Chemotherapy regimen			
Including IE	6	9	0.456
Not including IE	4	9	
Metastasis at final follow-up			
No	9	7	0.011*
Yes	1	11	

IE, ifosfamide and etoposide.
P-value was calculated using Fisher's exact test.
[a]Tumor sizes were evaluated in 24 patients.
*A probability of <0.05 was considered statistically significant.

possible explanation is the difference in the antibodies used. Berghuis et al. [8] have used two mAbs, HC10, and HCA2. HC10 was shown to react with HLA-B and C allele proteins, but barely with HLA-A [25]. In contrast, HCA2 preferentially reacts with HLA-A allele proteins except for HLA-A24 [26]. EMR8-5mAb used in the present study reacts all alleles of HLA-A, B, and C, including HLA-A24 [12,25]. Because HLA-A24 is shared by nearly half of Japanese and 17% of Caucasians [27], one analysis including HLA-A24 and the other analysis excluding HLA-A24 could show different results. In addition, differences in distribution of HLA types and fusion gene subtypes between the study groups could also affect the prognostic impact of HLA class I expression. In the present study, well-known prognostic factors of ESFTs such as tumor size, stage, and surgical margin have also shown significant prognostic impact, supporting the validity of our patient population.

Down-regulation of HLA class I molecule in tumor cells serves as a major mechanism of escaping from both natural immune surveillance and T cell-based immunotherapy [25,28]. Nevertheless none of the immunotherapy trials including those in patients with ESFT [29,30] have yet examined the status of HLA class I in the corresponding tumors. In the study by Mackall et al. [29] with translocation breakpoint peptide vaccines in 20 patients with ESFT, immune responses to the peptide vaccines were noted in 39% of the participants. The efficacy of those therapeutic vaccines can be further improved by restoration of HLA class I expression on tumor cells. In this regard, Berghuis et al.[8] reported that stimulations with interferon gamma have increased HLA class I expression in all six Ewing's sarcoma cell lines examined. Restoration of HLA class I expression can also be achieved with histone deacetylation inhibitors such as tricostatin-A and valporoic acid, provided that loss of HLA class I is due to reduced DNA methylation [25].

In conclusion, we revealed for the first time that the status of HLA class I expression affects the survival of patients with ESFT. This emphasizes the importance of HLA class I molecules in natural and therapeutic immune surveillance in patients with ESFT.

REFERENCES

1. Bernstein M, Kovar H, Paulussen M, et al.: Ewing's sarcoma family of tumors: Current management. Oncologist 2006;11:503–519.
2. Bernstein ML, Devidas M, Lafreniere D, et al.: Intensive therapy with growth factor support for patients with Ewing tumor metastatic at diagnosis: Pediatric Oncology Group/Children's Cancer Group Phase II Study 9457–a report from the Children's Oncology Group. J Clin Oncol 2006;24:152–159.
3. Miser JS, Goldsby RE, Chen Z, et al.: Treatment of metastatic Ewing sarcoma/primitive neuroectodermal tumor of bone: Evaluation of increasing the dose intensity of chemotherapy – A report from the Children's Oncology Group. Pediatr Blood Cancer 2007;49:894–900.
4. Gattinoni L, Powell DJ, , Rosenberg SA, et al.: Adoptive immunotherapy for cancer: Building on success. Nat Rev Immunol 2006;6:383–393.
5. Melief CJ, Toes RE, Medema JP, et al.: Strategies for immunotherapy of cancer. Adv Immunol 2000;75:235–282.
6. Cabrera T, Maleno I, Collado A, et al.: Analysis of HLA class I alterations in tumors: Choosing a strategy based on known patterns of underlying molecular mechanisms. Tissue Antigens 2007;69: 264–268.
7. Marincola FM, Jaffee EM, Hicklin DJ, et al.: Escape of human solid tumors from T-cell recognition: Molecular mechanisms and functional significance. Adv Immunol 2000;74:181–273.
8. Berghuis D, de Hooge AS, Santos SJ, et al.: Reduced human leukocyte antigen expression in advanced-stage Ewing sarcoma: Implications for immune recognition. J Pathol 2009;218:222–231.
9. Kikuchi E, Yamazaki K, Torigoe T, et al.: HLA class I antigen expression is associated with a favorable prognosis in early stage non-small cell lung cancer. Cancer Sci 2007;98:1424–1430.
10. Kitamura H, Honma I, Torigoe T, et al.: Down-regulation of HLA class I antigen is an independent prognostic factor for clear cell renal cell carcinoma. J Urol 2007;177:1269–1272 (discussion 1272).
11. Mizukami Y, Kono K, Maruyama T, et al.: Downregulation of HLA Class I molecules in the tumour is associated with a poor prognosis in patients with oesophageal squamous cell carcinoma. Br J Cancer 2008;99:1462–1467.
12. Tsukahara T, Kawaguchi S, Torigoe T, et al.: Prognostic significance of HLA class I expression in osteosarcoma defined by anti-pan HLA class I monoclonal antibody, EMR8-5. Cancer Sci 2006;97:1374–1380.
13. Urano F, Umezawa A, Yabe H, et al.: Molecular analysis of Ewing's sarcoma: Another fusion gene, EWS-E1AF, available for diagnosis. Jpn J Cancer Res 1998;89:703–711.
14. Enneking WF: A system of staging musculoskeletal neoplasms. Clin Orthop Relat Res 1986;204:9–24.
15. Jaffe N, Paed D, Traggis D, et al.: Improved outlook for Ewing's sarcoma with combination chemotherapy (vincristine, actinomycin D and cyclophosphamide) and radiation therapy. Cancer 1976;38:1925–1930.
16. Nesbit ME , Perez CA, Tefft M, et al.: Multimodal therapy for the management of primary, nonmetastatic Ewing's sarcoma of bone: An Intergroup Study. Natl Cancer Inst Monogr 1981;56:255–262.
17. Wilbur JR, Sutow WW, Sullivan MP, et al.: Chemotherapy of sarcomas. Cancer 1975;36:765–769.
18. Rosen G: Current management of Ewing's sarcoma. Prog Clin Cancer 1982;8:267–282.
19. Tanaka K, Kawamoto H, Saito I, et al.: Preoperative and postoperative chemotherapy with ifosfamide and adriamycin for adult high-grade soft-tissue sarcomas in the extremities: Japan Clinical Oncology Group Study JCOG0304. Jpn J Clin Oncol 2009;39: 271–273.
20. Grier HE, Krailo MD, Tarbell NJ, et al.: Addition of ifosfamide and etoposide to standard chemotherapy for Ewing's sarcoma and primitive neuroectodermal tumor of bone. N Engl J Med 2003; 348:694–701.
21. Obata H, Ueda T, Kawai A, et al.: Clinical outcome of patients with Ewing sarcoma family of tumors of bone in Japan: The Japanese Musculoskeletal Oncology Group cooperative study. Cancer 2007; 109:767–775.
22. Kaneko M, Nishihira H, Mugishima H, et al.: Stratification of treatment of stage 4 neuroblastoma patients based on N-myc amplification status. Study Group of Japan for Treatment of Advanced Neuroblastoma, Tokyo, Japan. Med Pediatr Oncol 1998;31:1–7.
23. Yabe H, Tsukahara T, Kawaguchi S, et al.: Overexpression of papillomavirus binding factor in Ewing's sarcoma family of tumors conferring poor prognosis. Oncol Rep 2008;19:129–134.
24. Kawaguchi S, Wada T, Nagoya S, et al.: Extraskeletal myxoid chondrosarcoma: A Multi-Institutional Study of 42 Cases in Japan. Cancer 2003;97:1285–1292.
25. Sato N, Hirohashi Y, Tsukahara T, et al.: Molecular pathological approaches to human tumor immunology. Pathol Int 2009;59:205–217.
26. Seitz C, Uchanska-Ziegler B, Zank A, et al.: The monoclonal antibody HCA2 recognises a broadly shared epitope on selected classical as well as several non-classical HLA class I molecules. Mol Immunol 1998;35:819–827.
27. Gotoh M, Takasu H, Harada K, et al.: Development of HLA-A2402/K(b) transgenic mice. Int J Cancer 2002;100:565–570.
28. Khong HT, Restifo NP: Natural selection of tumor variants in the generation of "tumor escape" phenotypes. Nat Immunol 2002;3: 999–1005.
29. Mackall CL, Rhee EH, Read EJ, et al.: A pilot study of consolidative immunotherapy in patients with high-risk pediatric sarcomas. Clin Cancer Res 2008;14:4850–4858.
30. Suminoe A, Matsuzaki A, Hattori H, et al.: Immunotherapy with autologous dendritic cells and tumor antigens for children with refractory malignant solid tumors. Pediatr Transplant 2009;13: 746–753.

EMBO
reports

scientific report

The IRE1α–XBP1 pathway is essential for osteoblast differentiation through promoting transcription of *Osterix*

Takahide Tohmonda[1,2], Yoshiteru Miyauchi[2], Rajarshi Ghosh[3], Masaki Yoda[1,2], Shinichi Uchikawa[2], Jiro Takito[2], Hideo Morioka[2], Masaya Nakamura[2], Takao Iwawaki[4,5], Kazuhiro Chiba[1,2], Yoshiaki Toyama[2], Fumihiko Urano[3] & Keisuke Horiuchi[1,2+]

[1]Department of Anti-aging Orthopedic Research, [2]Department of Orthopedic Surgery, School of Medicine, Keio University, Tokyo, Japan, [3]Program in Gene Function and Expression and Program in Molecular Medicine, University of Massachusetts Medical School, Worcester, Massachusetts, USA, [4]Iwawaki Initiative Research Unit, Advanced Science Institute, RIKEN, Wako, and [5]PRESTO, Japan Science and Technology Agency, Saitama, Japan

During skeletal development, osteoblasts produce large amounts of extracellular matrix proteins and must therefore increase their secretory machinery to handle the deposition. The accumulation of unfolded protein in the endoplasmic reticulum induces an adoptive mechanism called the unfolded protein response (UPR). We show that one of the most crucial UPR mediators, inositol-requiring protein 1α (IRE1α), and its target transcription factor X-box binding protein 1 (XBP1), are essential for bone morphogenic protein 2-induced osteoblast differentiation. Furthermore, we identify *Osterix* (*Osx*, a transcription factor that is indispensible for bone formation) as a target gene of XBP1. The promoter region of the *Osx* gene encodes two potential binding motifs for XBP1, and we show that XBP1 binds to these regions. Thus, the IRE1α–XBP1 pathway is involved in osteoblast differentiation through promoting *Osx* transcription.

Keywords: IRE1α; osteoblast differentiation; *Osterix*; unfolded protein response; XBP1

EMBO *reports* (2011) **12**, 451–457. doi:10.1038/embor.2011.34

[1]Department of Anti-aging Orthopedic Research,
[2]Department of Orthopedic Surgery, School of Medicine, Keio University, 35 Shinanomachi, Shinjuku-ku, Tokyo 160-8582, Japan
[3]Program in Gene Function and Expression and Program in Molecular Medicine, University of Massachusetts Medical School, Worcester, Massachusetts 01605, USA
[4]Iwawaki Initiative Research Unit, Advanced Science Institute, RIKEN, 2-1 Hirosawa, Wako, Saitama 351-0198, Japan
[5]PRESTO, Japan Science and Technology Agency, 4-1-8 Honcho Kawaguchi, Saitama 332-0021, Japan
+Corresponding author. Tel: +81 3 5363 3812; Fax: +81 3 3353 6597; E-mail: horiuchi@z3.keio.jp

Received 29 August 2010; revised 31 January 2011; accepted 1 February 2011; published online 18 March 2011

INTRODUCTION

To manage the burden of protein synthesis, cells augment the folding and secretory capacity of the endoplasmic reticulum (ER) in response to the accumulation of misfolded proteins. This system, known as the unfolded protein response (UPR), is a highly conserved cellular mechanism in eukaryotic cells. In mammalian cells, there are three classes of ER stress transducers involved in the UPR including inositol-requiring protein 1α (IRE1α), activating transcription factor 6 (ATF6) and pancreatic ER kinase (PERK), and their functions in the UPR have been a subject of intensive study in the past decade (Rutkowski & Kaufman, 2004; Xu *et al*, 2005; Ron & Walter, 2007; Hetz & Glimcher, 2009).

The activation of the UPR is especially important in cells specialized to secrete proteins including plasma cells, endocrine cells and osteoblasts. Past studies have shown that PERK (Zhang *et al*, 2002) and OASIS (old astrocyte specifically induced substance), an ATF6 homologue (Murakami *et al*, 2009), are involved in skeletal development. However, a potential role for IRE1α in osteoblast differentiation remains uninvestigated. IRE1α is a type-1 transmembrane protein harbouring both a kinase domain and an endoribonuclease domain. The former is involved in the recruitment of tumour necrosis factor receptor-associated factor 2 (TRAF2)—which in turn activates JUN amino-terminal kinase (JNK)—and the latter is involved in the processing of X-box binding protein 1 (XBP1) mRNA. The consequences of JNK activation through IRE1α signalling are not fully understood; however, it is probably involved in the initiation of autophagy (Ogata *et al*, 2006) and in the promotion of apoptosis (Yoneda *et al*, 2001). XBP1 derived from spliced *Xbp1* mRNA (XBP1s) translocates to the nucleus and binds to UPR elements to induce the transcription of a variety of UPR genes that mainly function to alleviate ER stress (Yoshida *et al*, 2001; Acosta-Alvear *et al*, 2007). Mice lacking IRE1α or XBP1 were embryonically lethal and died

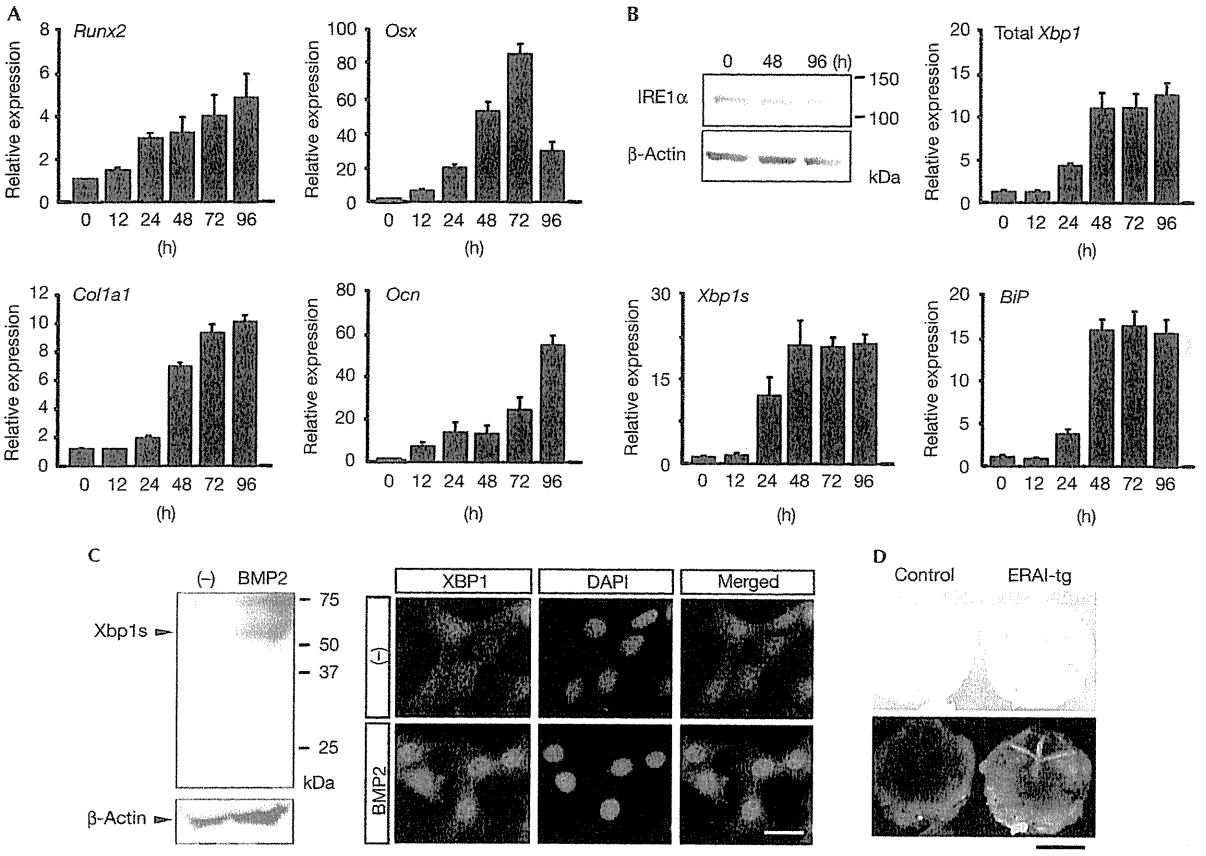

Fig 1 | *Xbp1* and *BiP* transcripts are upregulated during BMP2-induced osteoblast differentiation. Wild-type MEFs were incubated in the presence of BMP2 (200 ng/ml) for the designated time period. The expression levels of the transcripts for (**A**) osteoblast differentiation markers and (**B**) UPR-related genes were analysed by quantitative RT–PCR and western blot analysis (IRE1α). The expression level of each gene at baseline was set to one. (**C**) Western blot analysis (left panel) and immunostaining (right panel) of XBP1 in BMP2-treated or untreated (−) MEFs. Scale bar, 20 μm. (**D**) Fluorescent activity in BMP2 (500 ng/ml)-treated calvariae collected from control and ERAI-transgenic (ERAI-tg) newborn mice. Upper panel, light image; lower panel, fluorescence image. Scale bar, 3 mm. BMP2, bone morphogenic protein 2; ERAI, endoplasmic reticulum stress-activated indicator; IRE1α, inositol-requiring protein 1α; MEF, mouse embryonic fibroblast; RT, reverse transcription; UPR, unfolded protein response; XBP1, X-box binding protein 1.

at around 9.5–11.5 or 11.5–14.5 days post-coitum (dpc), respectively, supporting the idea that these genes are important *in vivo* (Reimold *et al*, 2000; Urano *et al*, 2000).

We investigated the potential role of IRE1α in osteoblast differentiation and found that the IRE1α–XBP1 pathway is essential for bone morphogenic protein 2 (BMP2)-induced osteoblast differentiation. Moreover, we identified *Osterix* (*Osx*)—one of the essential transcription factors for osteoblast differentiation (Nakashima *et al*, 2002)—as a target gene for XBP1s. In addition, we found that thapsigargin, a potent inducer of ER stress, can promote *Osx* transcription in BMP2-treated fibroblasts and in an osteoblast cell line—MC3T3-E1—in an IRE1α–XBP1-dependent manner. Taken together, these observations show a previously unknown relationship between the IRE1α–XBP1 pathway and *Osx*, and might provide new insights into the mechanisms underlying UPR and skeletal development.

RESULTS AND DISCUSSION

To examine the possible involvement of IRE1α signalling in osteoblast-differentiation, we performed *in vitro* osteoblast-differentiation experiments using mouse embryonic fibroblasts (MEFs) and recombinant BMP2, which is known to stimulate osteogenic differentiation processes in undifferentiated fibroblasts *in vitro*. The expression levels of two transcription factors that are essential for osteoblast differentiation, *Runx2* and *Osx* (Komori *et al*, 1997; Nakashima *et al*, 2002), and the bone extracellular matrix proteins COL1A1 and osteocalcin (OCN; markers for early and late stages of osteoblast differentiation, respectively), were evaluated to monitor the degree of differentiation. The expression levels of these osteoblastic markers in the MEFs—which were almost undetectable when cultured in maintenance medium—were significantly increased by the addition of BMP2 (Fig 1A). By contrast, the expression level of IRE1α showed no change during the course of the experiment (Fig 1B). However, we found that mRNA expression levels of total *Xbp1* (including both unspliced (*Xbp1u*) and spliced *Xbp1* (*Xbp1s*) mRNA), *Xbp1s* and *BiP/GRP78* chaperone were significantly upregulated, indicating that the UPR was induced by BMP2 in MEFs, probably to deal with the increase in protein synthesis that is known to occur in these conditions. There was also an increase in the expression

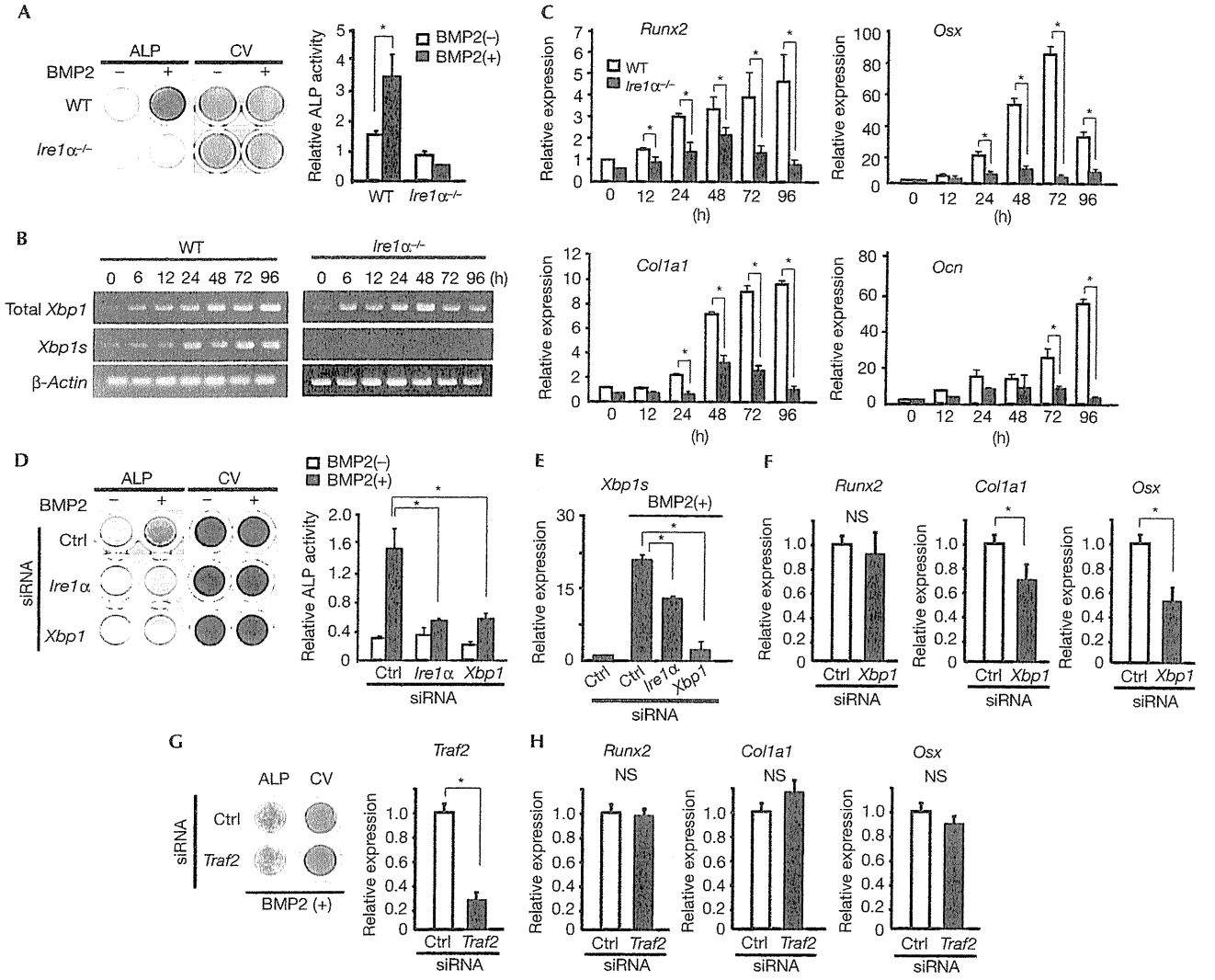

Fig 2 | The IRE1–XBP1, but not the IRE1–TRAF2, pathway is required for BMP2-induced osteoblast differentiation. (**A**) Wild-type and *Ire1α*$^{-/-}$ MEFs were incubated in the presence or absence of BMP2 (200 ng/ml) for 48 h. ALP activity was evaluated by cell staining with BCIP/NBT or by colorimetry (right panel) as described in the supplementary methods online. Cell staining with crystal violet (CV) showed a similar amount of cells in each well. (**B**) mRNA expressions of total *Xbp1* and *Xbp1s* in BMP2-treated wild-type and *Ire1α*$^{-/-}$ MEFs. (**C**) Quantitative analysis of the transcripts of osteoblast markers in BMP2-treated wild-type and *Ire1α*$^{-/-}$ MEFs. The expression level of each gene in wild-type MEFs at baseline was set to one. (**D**) Wild-type MEFs treated with control (Ctrl) *Ire1α*- or *Xbp1*-siRNA were incubated with or without BMP2 for 48 h. ALP activity was evaluated by cell staining (left panel) and colorimetry (right panel). (**E**) Quantitative analysis of *Xbp1s* in siRNA-introduced MEFs incubated with or without BMP2. (**F**) Quantitative analysis of the transcripts of osteoblast markers in *Xbp1*-siRNA-treated wild-type MEFs incubated in the presence of BMP2 for 48 h. (**G**) No difference in ALP activity between control (Ctrl) and *Traf2*-siRNA-treated wild-type MEFs incubated with BMP2 for 48 h (left panel) was observed. Quantitative PCR analysis showed a significant decrease in *Traf2* transcript levels in *Traf2*-siRNA-treated MEFs (right panel). (**H**) Quantitative PCR analysis of osteoblast markers showed no difference between control (Ctrl) and *Traf2*-siRNA-treated wild-type MEFs incubated with BMP2. The expression level of each gene in the control siRNA-transfected MEFs was set to one. *$P<0.05$. ALP, alkaline phosphatase; BMP2, bone morphogenic protein 2; Ctrl, control; IRE1α, inositol-requiring protein 1α; MEF, mouse embryonic fibroblast; NS, not significant; Ocn, Osteocalcin; Osx, Osterix; RT, reverse transcription; siRNA, small-interfering RNA; TRAF, tumour necrosis factor receptor-associated factor 2; UPR, unfolded protein response; XBP1, X-box binding protein 1.

levels of other UPR-related genes, including *Gadd34*, *Chop/Gadd153*, *Ero1a* and *Wfs1* (data not shown). In addition, we found that BMP2 treatment can upregulate the expression of genes in the other branches of ER stress inducers (PERK–ATF4 and ATF6; supplementary Fig S1 online). The increase in the level of XBP1 protein was also confirmed by western blot (Fig 1C, left panel), and immunocytochemistry of XBP1 in BMP2-treated MEFs showed an accumulation of XBP1 protein in the nucleus (Fig 1C, right panel). The processing of *Xbp1* in differentiating osteoblasts was also evaluated by using ER stress-activated indicator (ERAI)-transgenic

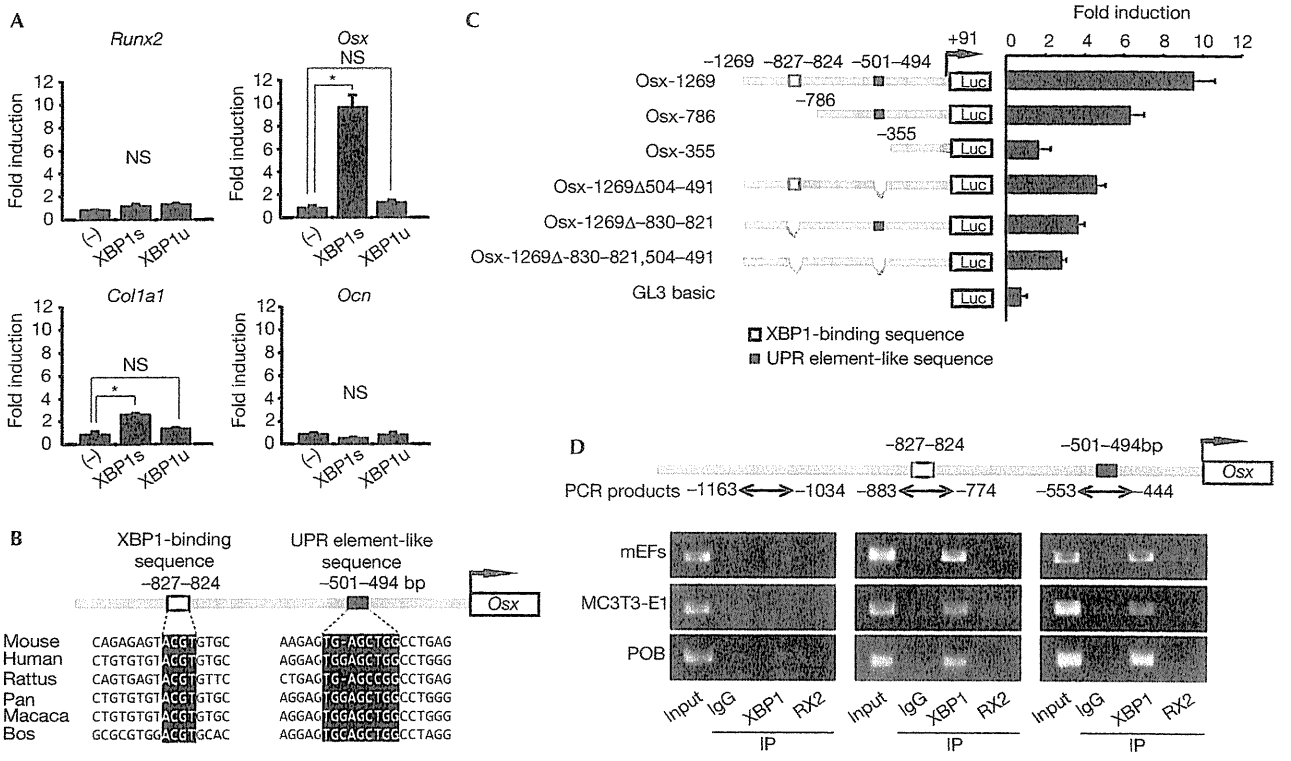

Fig 3 | XBP1 promotes *Osterix* transcription. (**A**) Reporter assays using the *Runx2*, *Osx*, *Col1a1* and *Ocn* promoter constructs. Mouse embryonic fibroblast cell line C3H10T1/2 was co-transfected with the indicated reporter constructs and an empty vector (−) or with an expression vector bearing either XBP1s or XBP1u complementary DNA. $^*P<0.05$. (**B**) Comparison of XBP1-binding sequence and UPR element-like sequence in the promoter region of the *Osx* genome between species. (**C**) Schematic representations of the *Osx* reporter constructs and the mutants (left panel). Reporter assays using the indicated reporter construct and an expression vector bearing XBP1s complementary DNA (right panel). Luciferase activity of the empty reporter construct (−)-transfected cells was set to one. (**D**) Schematic representation of the *Osx* promoter region and the expected PCR products (upper panel). Chromatin immunoprecipitation assays using a control rabbit IgG, XBP1 antibody or RUNX2 antibody (RX2, used as a negative control; lower panels). A set of primers that amplifies the region outside the putative binding sites was used as a negative control for the experiment. IgG, immunoglobulin G; IP, immunoprecipitation; mEF, mouse embryonic fibroblast; NS, not significant; Ocn, Osteocalcin; Osx, Osterix; POB, primary osteoblasts; UPR, unfolded protein response; XBP1, X-box binding protein 1; XBP1s, spliced X-box binding protein 1; XBP1u, unspliced X-box binding protein 1.

mice (Iwawaki *et al*, 2004), in which fluorescent protein is induced on activation of IRE1α. As shown in Fig 1D, there was a significant increase in fluorescence activity in the BMP2-treated calvarial bone collected from newborn ERAI-transgenic mice, especially in the junction of the sagittal and coronal sutures, where bone formation is achieved through direct differentiation of mesenchymal cells to osteoblasts. This observation illustrates that *Xbp1* transcripts are processed in the activated osteoblasts.

Next, we used MEFs lacking IRE1α to investigate how the absence of IRE1α in MEFs would affect their osteoblast-differentiation capacity and the production of extracellular matrix proteins. As shown in Fig 2A, the addition of BMP2 significantly increased alkaline phosphatase (ALP) activity in wild-type MEFs, compared with minimal or no increase in *Ire1α*$^{-/-}$ MEFs. These results indicate that BMP2-induced osteoblast differentiation is hampered by the absence of IRE1α. The absence of *Xbp1s* mRNA expression in *Ire1α*$^{-/-}$ MEFs was confirmed by reverse transcription (RT)–PCR (Fig 2B). A time course expression analysis of the aforementioned osteoblast markers by quantitative RT–PCR in BMP2-treated MEFs showed reduced expression in *Ire1α*$^{-/-}$ MEFs, compared with control MEFs (Fig 2C). The expression levels of other osteoblast markers—including bone sialoprotein, osteopontin and osteonectin—were also significantly reduced in *Ire1α*$^{-/-}$ MEFs, compared with control MEFs (supplementary Fig S2 online). As it is also conceivable that the hampered osteoblast differentiation in *Ire1α*$^{-/-}$ MEFs was derived from an increase in apoptosis, we evaluated the apoptosis in BMP2-treated *Ire1α*$^{-/-}$ and wild-type MEFs. As expected, there was an increase in the apoptosis rate in *Ire1α*$^{-/-}$ MEFs compared with wild-type MEFs; however, the overall ratio of the apoptotic cell rate was low (1.7% and 3.5% in wild-type and *Ire1α*$^{-/-}$ MEFs, respectively), suggesting that the increased apoptosis in the absence of IRE1α was not the primary cause for the defect in differentiation (supplementary Fig S3 online). Notably, even in the absence of IRE1α, there was a transient increase (peaking at around 48 h) in the expression levels of *Runx2* and *Col1a1* after BMP2 treatment, whereas the expression levels of *Osx* and *Ocn* (late-stage markers of osteoblast differentiation) remained almost unchanged. Taken

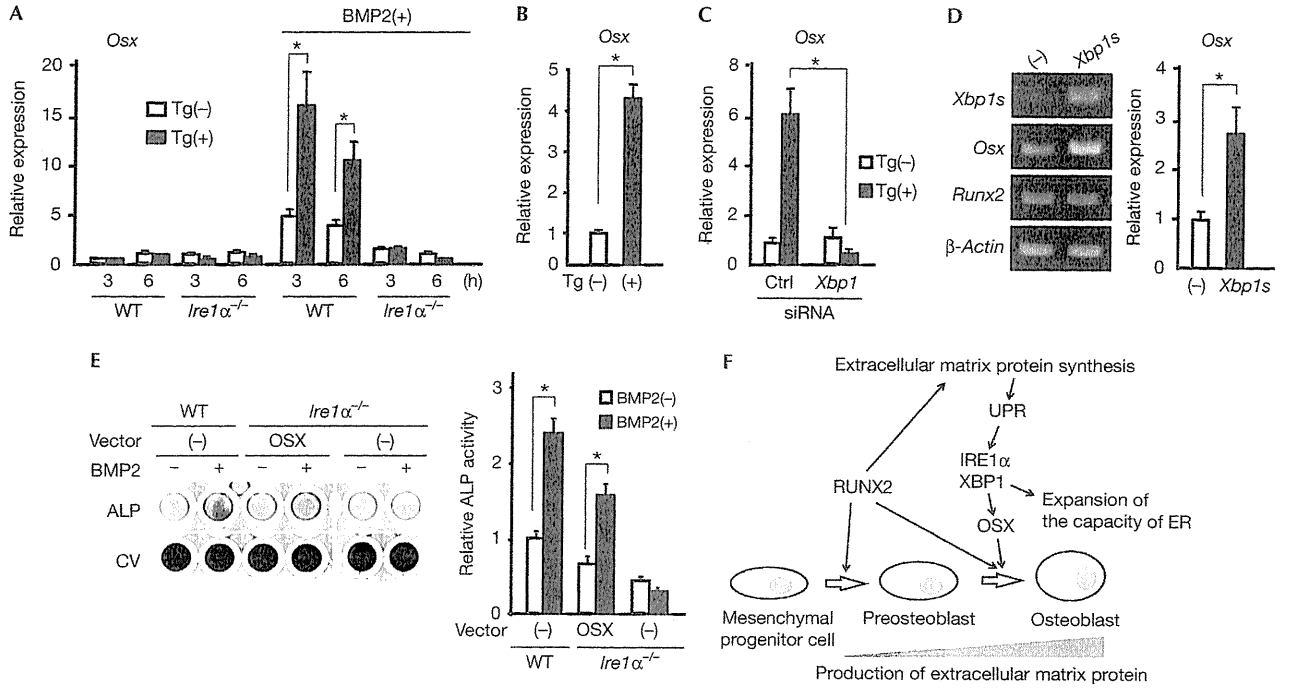

Fig 4 | *Osterix* transcription is induced by thapsigargin in BMP2-treated mouse embryonic fibroblasts and MC3T3-E1 cells. (**A**) Non-pretreated or BMP2-pretreated (BMP(+)) wild-type and *Ire1α*$^{-/-}$ MEFs were incubated with or without thapsigargin for 3 or 6 h. The expression level of the *Osx* gene was evaluated by quantitative PCR. (**B**) Quantitative analysis of *Osx* transcripts in MC3T3-E1 cells incubated with or without thapsigargin (Tg) for 3 h. (**C**) Quantitative analysis of *Osx* transcripts in MC3T3-E1 cells treated with control or *Xbp1*-siRNA in the presence or absence of thapsigargin. (**D**) RT–PCR analysis of *Xbp1s*, *Osx* and *Runx2* transcripts in the control vector (−) or XBP1s-expression vector-introduced MC3T3-E1 cells (left panel). The expression level of *Osx* was also evaluated by quantitative RT–PCR (right panel). (**E**) Wild-type and *Ire1α*$^{-/-}$ MEFs transfected with a control (−) or OSX expression vector (OSX) were incubated in the presence or absence of BMP2 (200 ng/ml) for 5 days. ALP activity was evaluated by cell staining with BCIP/NBT and by colorimetry (right panel). *$P<0.05$. (**F**) A schematic model showing the role of IRE1α–XBP1-mediated UPR in osteoblast differentiation. ALP, alkaline phosphatase; BMP2, bone morphogenic protein 2; CV, crystal violet; ER, endoplasmic reticulum; IRE1α, inositol-requiring protein 1α; Ocn, Osteocalcin; Osx, Osterix; RT, reverse transcription; UPR, unfolded protein response; siRNA, small interfering RNA; XBP1, X-box binding protein 1.

together, these observations indicate that the maturation of osteoblasts is inhibited in the absence of IRE1α, whereas the initial stage of differentiation—in which undifferentiated mesenchymal cells commit to the osteoblast lineage—is not affected.

It has been shown previously that IRE1α not only processes *Xbp1* mRNA, but can also activate stress-induced JNK through recruitment of TRAF2 (Urano *et al*, 2000). Next, we asked which of these pathways is more involved in BMP2-induced osteoblast differentiation. We used small interfering RNA (siRNA)-mediated gene silencing to suppress the expression of XBP1 and TRAF2 in wild-type MEFs and subjected these cells to *in vitro* osteoblast-differentiation experiments. In *Ire1α*- and *Xbp1*-siRNA-transfected MEFs, the increase in ALP activity after BMP2 treatment was reduced to a level comparable to that observed in *Ire1α*$^{-/-}$ MEFs (Fig 2D). The reduction in the amount of *Xbp1s* mRNA was confirmed by quantitative RT–PCR (Fig 2E). In addition, we found that the mRNA expression levels of *Col1a1* and *Osx* were significantly reduced, whereas that of *Runx2* remained unaltered (Fig 2F). Conversely, introduction of *Traf2*-siRNA into MEFs had little effect on their potential to induce ALP after BMP2 treatment (Fig 2G, left panel). The suppression of the transcript level of *Traf2* in siRNA-transfected MEFs was confirmed by quantitative RT–PCR (Fig 2G, right panel). Consistently, there was no change in mRNA expression levels in any of the osteoblast markers in *Traf2*-siRNA-treated cells (Fig 2H). Taken together, these observations suggest that the IRE1α–XBP1, but not the IRE1α–TRAF2, pathway is essential for BMP2-induced osteoblast differentiation.

To gain insight into the regulatory mechanism underlying IRE1α–XBP1 and osteoblast differentiation, we performed a reporter assay using reporter constructs carrying the promoter of *Runx2*, *Osx*, *Col1a1* and *Ocn*. Unexpectedly, we found that reporter activity was highly induced in cells transfected with an *Osx*-reporter vector and XBP1s expression vector, and to a lesser extent in the cells transfected with a *Col1a1*-reporter vector (Fig 3A). By contrast, there was no change in reporter activity in the cells transfected with a *Runx2*- or *Ocn*-reporter vector. Introduction of the unspliced version of XBP1—which could potentially interfere with the activity of XBP1s (Yoshida *et al*, 2006)—had no effect on reporter activity in the cells transfected with any of the four reporter constructs. In addition, co-transfection of ATF4 (which functions downstream of PERK) or ATF6 expression vector with the *Osx*-reporter construct did not show any change

in reporter activity (data not shown). Interestingly, comparative genomic sequence analysis revealed that the promoter region of *Osx* encodes a UPR element (TGACGTGG/A)-like sequence (TGAGCTGG; Yoshida *et al*, 2001) and an XBP1-binding sequence (ACGT; Acosta-Alvear *et al*, 2007), which are highly conserved among species (Fig 3B). On the basis of these sequence data, we generated several mutant reporter constructs and performed a luciferase assay. As shown in Fig 3C, the shorter reporter constructs—which lack one (*Osx* −786) or both (*Osx* −355) of the aforementioned putative binding motifs—showed a decrease in luciferase activity, compared with the full-length construct (*Osx* −1269). Furthermore, the mutant constructs—which lack either one (*Osx* 1269 Δ504–491 and *Osx* −1269 Δ−830–821) or both (*Osx* −1269 Δ−830–821, 504–491) binding motifs—also showed a significant decrease in the XBP1s-driven luciferase activity. Chromatin immunoprecipitation assays confirmed that XBP1 binds to the promoter region of *Osx* containing either one of the putative binding motifs in MEFs, MC3T3-E1 cells and primary osteoblasts from wild-type newborn mice (Fig 3D).

The observations that XBP1s promotes *Osx* transcription in the reporter assay led us to ask whether ER stress alone is capable of inducing *Osx* transcription. We repeated the reporter assays using the aforementioned *Osx* reporter constructs and found that ER stress induced by thapsigargin is able to promote *Osx* reporter activity (supplementary Fig S4 online). Furthermore, this activity was abolished in *Ire1α*$^{-/-}$ MEFs, in which no *Xbp1s* mRNA is expressed (Fig 2B), indicating that ER stress-induced *Osx* reporter activity is dependent on IRE1α, presumably involving IRE1a-mediated induction of XBP1s. Next, we incubated wild-type and *Ire1α*$^{-/-}$ MEFs with thapsigargin for 3 or 6 h and then examined the transcript level of *Osx* by quantitative RT–PCR. As shown in Fig 4A, there was no change in *Osx* transcripts in either wild-type or *Ire1α*$^{-/-}$ MEFs; however, when the cells were preincubated with BMP2 for 16 h, the addition of thapsigargin significantly induced the *Osx* transcripts in wild-type, but not in *Ire1α*$^{-/-}$, MEFs. Furthermore, we found that treatment with thapsigargin alone was sufficient to promote *Osx* transcripts in a preosteoblastic cell-line, MC3T3-E1 (Fig 4B). The thapsigargin-induced *Osx* transcripts were abolished by gene silencing of *Xbp1* (Fig 4C), indicating that upregulation of *Osx* transcripts by thapsigargin is XBP1s-dependent. Consistently, overexpression of XBP1s was also capable of inducing *Osx* transcripts, but not those of *Runx2*, in MC3T3-E1 cells (Fig 4D). These observations suggest that after a cell differentiates into a preosteoblast, *Osx* becomes inducible by XBP1-dependent UPR signalling.

Finally, to consolidate our observations, we examined whether the introduction of *Osx* to *Ire1α*$^{-/-}$ MEFs could rescue the defect in BMP2-induced osteoblastic differentiation. As shown in Fig 4E, we found that enhanced expression of *Osx* can partly restore ALP activity in the BMP-treated *Ire1α*$^{-/-}$ MEFs, further supporting a functional link between the IRE1α–XBP1 pathway and *Osx*.

In summary, this study indicates that UPR has two functions during osteoblast differentiation: (i) to expand the capacity of the ER to cope with the increase in the production of extracellular matrix proteins, and to avoid the cells producing matrix proteins from apoptosis induced by ER overload (Hino *et al*, 2010); (ii) to stimulate *Osx* expression through the IRE1α–XBP1 pathway to promote the maturation of preosteoblasts into osteoblasts (Fig 4F). In comparison to *Runx2*, the functions and the molecular regulation of *Osx* are poorly understood, although both genes are equally indispensible for skeletogenesis (Komori, 2006; Karsenty, 2008). Therefore, the unexpected link between the IRE1α–XBP1 pathway and *Osx* identified here might shed new light on the understanding of the UPR and osteoblast differentiation.

METHODS

Cells and reagents. The generation of *Ire1α*$^{-/-}$ and wild-type MEFs was described previously (Urano *et al*, 2000). Primary osteoblasts were collected from the calvaria from 18.5 dpc wild-type embryos. Recombinant human BMP2 was purchased from Wako (Osaka, Japan). IRE1α antibody (14C10), XBP1 antibody (M-186), RUNX2 antibody (M-70) and actin antisera were from Cell Signaling, Santa Cruz (M-186 and M-70) and Sigma-Aldrich, respectively. *Ire1α*, *Xbp1*, *Traf2* and non-targeting control siRNA were purchased from Sigma Genosys.

Luciferase assay. Luciferase assay was performed using a dual luciferase assay system (Promega). pRL-SV40 (Promega) was used as a transfection efficiency control. The assays were performed 16 h after the transfection of reporter constructs and expression vectors. Transcriptional activity was expressed as a ratio of firefly:Renilla luciferase activity.

Chromatin immunoprecipitation assay. MC3T3-E1 cells, MEFs and primary osteoblasts were cultured in BMP2-supplemented medium for 72 h. The cells were fixed by 1% paraformaldehyde/phosphate-buffered saline for 10 min at 23 °C. Chromatin shearing and immunoprecipitation were performed using ChIP-IT Express Chromatin Immunoprecipitation Kits (Active Motif), as instructed by the manufacturer. The isolated DNA fragments were used as templates for PCR amplification (see Fig 3D for a schema showing the target region for PCR and supplementary Table S1 online for the PCR primers used in this study).

Statistical analysis. A student's *t*-test for two samples assuming equal variances was used to calculate *P*-values. *P*-values <0.05 were considered statistically significant. All experiments, including the reporter assay, quantitative RT–PCR and chromatin immunoprecipitation assay, were repeated at least three times. Error bars indicate standard deviation.

Detailed description of the constructs and the protocols for immunostaining, evaluation for ALP activity, *ex vivo* culture of calvariae and quantitative RT–PCR are provided in the supplementary information online.

Supplementary information is available at EMBO *reports* online (http://www.emboreports.org).

ACKNOWLEDGEMENTS

We thank Ms Shizue Tomita and Ms Kaori Sue for their technical assistance. This work was supported in part by the Takeda Science Foundation, Keio University Kanrinmaru project and MEXT KAKENHI (21390424).

CONFLICT OF INTEREST

The authors declare that they have no conflict of interest.

REFERENCES

Acosta-Alvear D, Zhou Y, Blais A, Tsikitis M, Lents NH, Arias C, Lennon CJ, Kluger Y, Dynlacht BD (2007) XBP1 controls diverse cell type- and condition-specific transcriptional regulatory networks. *Mol Cell* **27:** 53–66

Hetz C, Glimcher LH (2009) Fine-tuning of the unfolded protein response: assembling the IRE1α interactome. *Mol Cell* **35:** 551–561

Hino S *et al* (2010) Regulation of ER molecular chaperone prevents bone loss in a murine model for osteoporosis. *J Bone Miner Metab* **28:** 131–138

Iwawaki T, Akai R, Kohno K, Miura M (2004) A transgenic mouse model for monitoring endoplasmic reticulum stress. *Nat Med* **10:** 98–102

Karsenty G (2008) Transcriptional control of skeletogenesis. *Annu Rev Genomics Hum Genet* **9:** 183–196

Komori T (2006) Regulation of osteoblast differentiation by transcription factors. *J Cell Biochem* **99:** 1233–1239

Komori T *et al* (1997) Targeted disruption of Cbfa1 results in a complete lack of bone formation owing to maturational arrest of osteoblasts. *Cell* **89:** 755–764

Murakami T *et al* (2009) Signalling mediated by the endoplasmic reticulum stress transducer OASIS is involved in bone formation. *Nat Cell Biol* **11:** 1205–1211

Nakashima K, Zhou X, Kunkel G, Zhang Z, Deng JM, Behringer RR, de Crombrugghe B (2002) The novel zinc finger-containing transcription factor osterix is required for osteoblast differentiation and bone formation. *Cell* **108:** 17–29

Ogata M *et al* (2006) Autophagy is activated for cell survival after endoplasmic reticulum stress. *Mol Cell Biol* **26:** 9220–9231

Reimold AM *et al* (2000) An essential role in liver development for transcription factor XBP-1. *Genes Dev* **14:** 152–157

Ron D, Walter P (2007) Signal integration in the endoplasmic reticulum unfolded protein response. *Nat Rev Mol Cell Biol* **8:** 519–529

Rutkowski DT, Kaufman RJ (2004) A trip to the ER: coping with stress. *Trends Cell Biol* **14:** 20–28

Urano F, Wang X, Bertolotti A, Zhang Y, Chung P, Harding HP, Ron D (2000) Coupling of stress in the ER to activation of JNK protein kinases by transmembrane protein kinase IRE1. *Science* **287:** 664–666

Xu C, Bailly-Maitre B, Reed JC (2005) Endoplasmic reticulum stress: cell life and death decisions. *J Clin Invest* **115:** 2656–2664

Yoneda T, Imaizumi K, Oono K, Yui D, Gomi F, Katayama T, Tohyama M (2001) Activation of caspase-12, an endoplastic reticulum (ER) resident caspase, through tumor necrosis factor receptor-associated factor 2-dependent mechanism in response to the ER stress. *J Biol Chem* **276:** 13935–13940

Yoshida H, Matsui T, Yamamoto A, Okada T, Mori K (2001) XBP1 mRNA is induced by ATF6 and spliced by IRE1 in response to ER stress to produce a highly active transcription factor. *Cell* **107:** 881–891

Yoshida H, Oku M, Suzuki M, Mori K (2006) pXBP1(U) encoded in XBP1 pre-mRNA negatively regulates unfolded protein response activator pXBP1(S) in mammalian ER stress response. *J Cell Biol* **172:** 565–575

Zhang P, McGrath B, Li S, Frank A, Zambito F, Reinert J, Gannon M, Ma K, McNaughton K, Cavener DR (2002) The PERK eukaryotic initiation factor 2 alpha kinase is required for the development of the skeletal system, postnatal growth, and the function and viability of the pancreas. *Mol Cell Biol* **22:** 3864–3874

J Orthop Sci (2011) 16:443–450
DOI 10.1007/s00776-011-0091-x

ORIGINAL ARTICLE

Treatment of collagen-induced arthritis with recombinant plasminogen-related protein B: a novel inhibitor of angiogenesis

Koichiro Tanaka · Takeshi Morii · Lawrence Weissbach · Keisuke Horiuchi · Katsuhito Takeuchi · Yoshiaki Toyama · Hideo Morioka

Received: 17 October 2010 / Accepted: 14 April 2011 / Published online: 17 May 2011

Abstract
Background We have previously reported that recombinant human plasminogen-related protein B (rPRP-B), a putative 9-kDa protein that closely resembles the activation peptide of plasminogen, has shown significant inhibition of tumor growth through inhibition of angiogenesis. Based on recent reports suggesting a close relationship between rheumatoid arthritis (RA) and angiogenesis, we hypothesized that this compound would regulate inflammatory conditions in RA. The present study therefore tested the effects of rPRP-B in the treatment of collagen-induced arthritis (CIA) to elucidate the mechanisms underlying these effects.
Methods DBA/1J mice immunized with type II collagen to induce CIA were monitored to assess the effects of rPRP-B on clinical severity of the disease. Pathological changes in joints, including vessel formation and vascular endothelial growth factor (VEGF) production, were examined histologically. Bone destruction was radiologically evaluated. In vitro studies on the effects of rPRP-B on cell proliferation and production of VEGF in interleukin (IL)-1β or basic fibroblast growth factor (bFGF)-stimulated human synoviocytes were also performed.
Results Development of CIA was effectively inhibited by rPRP-B. Radiological examinations revealed that the protein reduced bone destruction in CIA. CIA-induced vessel formation and VEGF expression in vivo were also reduced. In vitro mechanistic studies demonstrated that rPRP-B affected human synoviocyte proliferation and VEGF production stimulated by IL-1β and bFGF.
Conclusions Given the ability to effectively promote multistep anti-angiogenic activities, including cell growth inhibition and cytokine regulation, rPRP-B represents a promising candidate for a novel therapeutic agent against RA.

K. Tanaka (✉) · K. Horiuchi · K. Takeuchi · Y. Toyama · H. Morioka
Department of Orthopaedic Surgery,
Keio University School of Medicine,
35 Shinanomachi, Shinjuku, Tokyo 160-8582, Japan
e-mail: koichiro@bd.mbn.or.jp

K. Horiuchi
e-mail: horiuchi@z3.keio.jp

K. Takeuchi
e-mail: ktakeuch@tcc.pref.tochigi.lg.jp

Y. Toyama
e-mail: toyama@sc.itc.keio.ac.jp

H. Morioka
e-mail: morioka@sc.itc.keio.ac.jp

T. Morii
Department of Orthopaedic Surgery, Kyorin University,
6-20-2 Shinkawa, Mitaka, Tokyo 181-8611, Japan
e-mail: t-morii@gb3.so-net.ne.jp

L. Weissbach
Sarcoma Molecular Biology Laboratory, Massachusetts General Hospital, 70 Blossom Street, MGR J 1115, Boston, MA 02114, USA
e-mail: lawrence.weissbach@gmail.com

Introduction

Plasminogen-related gene B (PRG-B) encodes a putative 9-kDa protein [plasminogen-related protein (PRP)-B] that closely resembles the activation peptide of plasminogen [1]. Messenger ribonucleic acid (mRNA) for PRG-B was originally discovered in cultured articular chondrocytes derived from human cartilage, one of the least vascular

tissues in the body [1]. We have previously analyzed the biological activity of recombinant PRP-B (rPRP-B) and have shown significant inhibition of tumor growth through inhibition of angiogenesis [2, 3]. Moreover, an in vitro model revealed a potential role of this protein in inhibiting angiogenesis by inhibiting endothelial cell proliferation, migration, and vessel formation through interaction with the cell surface $\alpha v\beta_3$ integrin in vitro [4]. Upregulated expression of this gene in several malignancies and inflammatory conditions has been confirmed, suggesting a role in the pathogenesis or regulation of both neoplastic and inflammatory conditions [3, 5].

Rheumatoid arthritis (RA) is a chronic inflammatory disease characterized by severe synovial inflammation, resulting in destruction of bone and cartilage and loss of structural integrity and normal joint function. Upregulation of pro-angiogenic mediators in RA patients suggests that angiogenesis is closely related to the progression of RA [6]. Although dramatic effects of biological agents, such as tumor necrosis factor (TNF)-alpha blockers, have recently been reported, criticisms of serious side effects, such as predispositions to tuberculosis, lymphoma, and progressive multifocal leukoencephalopathy and high cost, have been raised [7], indicating the need for substitute modalities for the treatment of RA. Anti-angiogenic therapy thus offers a promising candidate for the treatment of RA. The present study confirmed the biological activity of rPRP-B in inhibiting inflammatory conditions in the collagen-induced arthritis (CIA) mouse based on the hypothesis that anti-angiogenic activity of rPRP-B could regulate RA activity. In addition, analyses of biological activity of rPRP-B in an in vitro inflammatory model were performed to clarify the underlying mechanisms.

Materials and methods

Purification of recombinant protein

The cloning of PRG-B and characterization of a recombinant form of the bacterial-derived recombinant polyhistidine-tagged PRP-B have been described previously [2]. In brief, a human fetal liver cDNA library (kindly supplied by A. Bernards, Massachusetts General Hospital Cancer Center) constructed in λgt10 was screened by a standard procedure for PRG-B cDNA using a probe encompassing the Pgn intron D-homologous region in PRG-B. A recombinant fusion protein comprising recombinant PRG-B fused to an N-terminal hexahistidine tag was constructed, as described previously [8]. The endotoxin level in the rPRP-B preparation was determined using an Endosafe system (Charles River, Charleston, SC) [9].

Cell culture

Human fibroblast-like synoviocytes (HFLSs) were purchased from Cell Applications (San Diego, CA). Cells between passages 3 and 5 were used for experiments.

Cell proliferation assay

Proliferation of HFLSs with inflammatory cytokine stimulation and the effects of rPRP-B were monitored as described previously with some modifications [4, 10]. Concentration of rPRP-B was determined according to a previous study [4]. HFLSs were harvested for 24 h. After adding rPRP-B (5 μg/ml), cultures were treated with 5 ng/ml of bFGF (Oncogene Research Products, San Diego, CA) or IL-1β (PeproTech EC, London, UK). Following incubation, viable cells were detected using a CellTiter 96 AQueous spectrophotometric cell proliferation assay (Promega, Madison, WI).

Real-time polymerase chain reaction (real-time PCR)

We investigated the expression of vascular endothelial growth factor (VEGF) mRNA in HFLSs with or without rPRP-B treatment by real-time PCR using a Light Cycler system (Roche Diagnostic, Basel, Switzerland). The mRNA expression levels were normalized to GAPDH mRNA levels.

Enzyme-linked immunosorbent assay (ELISA)

We plated HFLSs, and cultures were treated with bFGF or IL-1β with or without rPRP-B. Levels of VEGF in cell culture supernatants were measured using a Quantikine immunoassay kit for human VEGF (R&D Systems, Minneapolis, MN).

CIA mice

CIA was induced as described previously [11]. Briefly, male DBA/1J mice were injected intradermally at the base of the tail with chicken type II collagen (Chondrex, Redmond, WA) in acetic acid emulsified in Freund's complete adjuvant (Difco, Detroit, MI). At 21 days after primary immunization, mice were administered a booster injection of type II collagen. At 24 days after the first immunization, mice were divided into two groups ($n = 7$ each): a control group and a rPRP-B treatment group. Each group received subcutaneous injections of either control PBS or rPRP-B (5 mg/kg/day) once daily on days 24–34 after the first immunization. An immunization-free group ($n = 7$) was also included as a control. To evaluate the severity of arthritis, thickness of the hind paw was measured every

3 days using Vermier calipers by two investigators blinded to experimental groups. All mice were maintained under specific pathogen-free conditions. All animal experiments were approved by the Institutional Animal Care and Use Committee of the Keio University School of Medicine, and all experiments were conducted in accordance with the institutional ethical guidelines.

Histological assessment of arthritis

Mice with CIA from different groups were killed on day 43 after immunization. The hind paws of each mouse were removed and fixed in 10% formalin. Samples were decalcified, then embedded in paraffin. Tissues were divided into 4-μm sections and stained with hematoxylin and eosin. Histopathological grading of joint lesions was performed semiquantitatively on a scale from 0 to 3, as previously described [12]. The following criteria were examined: inflammatory infiltrate (0, none; 1, mild; 2, moderate; 3, severe infiltrate); synovial lesion (0, no lesion; 1, mild alteration; 2, moderate alteration; 3, severe/complete destruction of the synovia); cartilage destruction (0, none; 1, mild; 2, moderate; 3, severe destruction with loss or complete fragmentation of cartilage); and bone destruction (0, none; 1, mild destruction of subchondral bone; 2, moderate destruction; 3, severe destruction with loss of large areas of bone).

Immunohistochemistry

Primary antibodies comprised anti-mouse CD31 antibody (×400) (BD Biosciences Pharmingen) and anti-mouse VEGF antibody (×200) (Calbiochem). As a secondary antibody for CD31 staining, anti-rat biotin-labeled mouse antibody (×100) (DakoCytomation) was used. For VEGF staining, Histofine® Simple Stain MAX PO (Nichirei Biosciences, Tokyo, Japan) was used. Finally, the reactant was visualized using 3,3′-diaminobenzidine (DakoCytomation). The number of positive cells was counted in eight randomly selected high-power fields (×200) and plotted.

Radiological evaluation

Bone destruction near joints was evaluated using micro-computed tomography (CT) (Micro-focus 2D/3DX-ray CT scanning device, ScanXmate-E090S40, Iwaken, Tokyo, Japan): 32 kV; 151 μA; 4.7 W. The amputated hind paw including tarsal bones and metatarsal bones was used for this examination.

Statistical analysis

Representative values were determined as means of values obtained from each mouse in a group, and all values in the experimental groups were compared to untreated CIA mice. All results and measurements are expressed as mean ± standard deviation. Statistical comparisons between two groups were evaluated using the Mann-Whitney U test and the Kruskal-Wallis test. Values of $P < 0.05$ were considered statistically significant. All analyses were performed using JMP version 7.0.1 software (SAS Institute Japan, Tokyo, Japan).

Results

Human synoviocyte proliferation by bFGF or IL-1β was inhibited by PRP-B

We have previously confirmed the inhibitory effects of rPRP-B on bFGF-stimulated endothelial cell proliferation [4]. We thus speculated on the possible biological effects of the rPRP-B on bFGF-driven cell activity in synoviocytes. IL-1β is known as a cytokine that promotes synovitis under inflammatory conditions [13] and was used for stimulation of HFLS growth in the present study. rPRP-B significantly inhibited the cell proliferation of HFLSs under stimulation by both bFGF and IL-1β (Fig. 1).

rPRP-B significantly decreased the VEGF expression of bFGF or IL-1β stimulated HFLSs

The anti-angiogenic activity of rPRP-B [2] led to speculating about possible activity of the protein on VEGF expression in target cells. Expression levels of VEGF were found to be reduced by rPRP-B in the culture supernatants of both bFGF- and IL-1β-stimulated FLSs (Fig. 2).

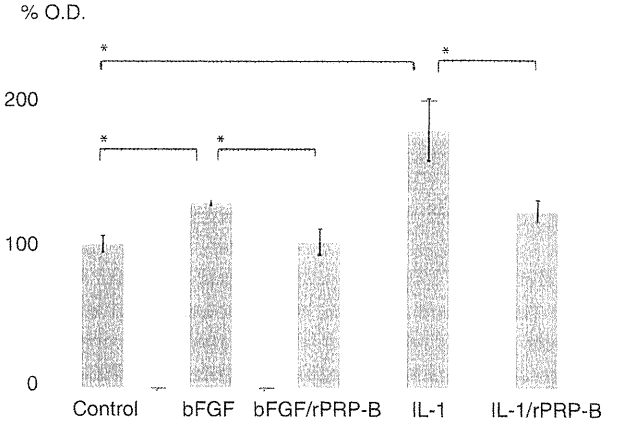

Fig. 1 HFLS proliferation with inflammatory cytokine stimulation and effects of rPRP-B. Significant reductions in cell proliferation were induced by administration of rPRP-B with both bFGF and IL-1 stimulation (*$P < 0.05$)